Bandwidth-Enhanced Compact Meander Printed Dipole Antenna

Chongyi Yue [1,2], Atef Elsherbeni [2], Veysel Demir [3], and Wenxing Li [1]

[1] Department of Information and Communication Engineering
Harbin Engineering University, Harbin, Heilongjiang 150001, China
yuechongyi@hrbeu.edu.cn, liwenxing@hrbeu.edu.cn

[2] College of Engineering and Computational Sciences
Colorado School of Mines, Golden, CO 80401, US
cyue@mines.edu, aelsherb@mines.edu

[3] Department of Electrical Engineering
Northern Illinois University, DeKalb, IL 60115, US
vdemir@niu.edu

Abstract ─ A miniaturization design of printed dipole antenna is proposed in this paper with enhanced operating bandwidth. As an example, three designs including a printed dipole, a meander dipole and a loop meander dipole, used in the wireless communication at 2.46 GHz are presented. The parameters regarding expanding bandwidth and reducing antenna size are discussed in details. These two antennas are modeled, simulated and optimized using HFSS and CEMS. Fabrication of the antennas are also performed. The simulation results and measurements show that the method proposed in this paper make the printed dipole more compact and bandwidth efficient.

Index Terms ─ Antenna miniaturization, meander antenna, wideband dipole antenna.

I. INTRODUCTION

With the expanding of the wireless terminals and hardware, the antenna miniaturization has been attracting more and more attention [1, 2]. Because the antennas are often integrated on a small circuit board and the space reserved for the antenna in the communication system such as the cell phones is usually smaller than one wavelength. The antenna elements printed on the substrate are generally a type of dipoles or monopoles and the design of electrically small antennas can be obtained by folding or meandering the antenna arm [3-5]. One of the main issues of reducing the antenna dimensions is the limitation of the bandwidth.

The expand of the bandwidth of printed dipoles is challenging. A previous study shows the 10 dB bandwidth of a dipole can be expanded from 2.9% to 4.8% at 2.43 GHz by folding the antenna [6], which is not very satisfactory.

In this paper, we focus on the better miniaturization and bandwidth extension of the printed dipole, thus three novel designs of printed dipole are proposed. With the intention to demonstrate the bandwidth enhancement, a printed dipole antenna (unfolded) operating at 2.46 GHz is first modeled and simulated. Then, in order to reduce the size of the antenna, a design of a meander antenna is introduced. This meander antenna has the same operating frequency as the printed dipole; however, this design reduces the size of the antenna arm by 30.6%. Another meander loop antenna is also designed afterwards. Although the size of the meander loop antenna is the same as the meander antenna mentioned above, the bandwidth of the meander loop antenna is increased by 43.5%.

The parameters in all the designs are discussed in details and the difference in the frequency performance due to the adjustment of the parameters are shown in the simulation. The software package Ansoft high-frequency structure simulator (HFSS) is used to numerically analysis all the designs. To verify the simulation results produced by HFSS, the home made software package CEMS [7], which is a 3D electromagnetic simulation tool based on the finite-difference time-domain method (FDTD), is employed to compute the return loss. The simulation results from these two simulation tools fit well. Fabrications and measurement of return loss of three antennas mentioned above are performed. The measurements and the simulation results have a good agreement.

II. PRINTED DIPOLE ANTENNA

In this part, a dipole antenna operating at 2.46 GHz is presented. The dipole is printed on both sides of a substrate with dimensions of 62 mm × 50 mm × 0.75 mm.

The front and back view of the printed dipole are shown in Fig. 1 (a) and Fig. 1 (b). The dielectric of the substrate has relative permittivity ε_r=2.2. The dipole arm is 1 mm wide and 24.5 mm long. The dipole arm on the front side is along negative z direction, while the arm on the back side is towards positive direction.

The HFSS with finite element method (FEM) kernel is employed for all the simulations in the research, and the FDTD software package CEMS (based on [7]) is used to verify the simulated results. One of advantages of using CEMS is that all the program can be running on the GPU, which has been proved to be quite efficient for the simulation process. In order to find more suitable designs for these three antennas, the optimetrics module in the HFSS is used to do the automate parametric sweeps, which allows us to get the appropriate parameters for each design more efficiently. The magnitude of S_{11} parameter from 2 GHz to 3 GHz is shown in Fig. 2. The printed dipole operates from 2.36 GHz to 2.57 GHz and the resonant frequency is centered at 2.46 GHz. The bandwidth of the antenna is 8.53%. It can be observed that the curves of the return loss produced by these two simulation tools match very well, which indicates that the simulation results are accurate and believable.
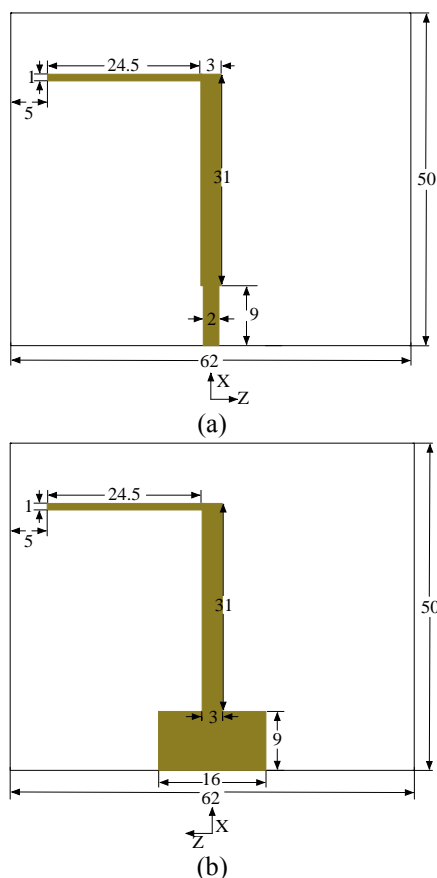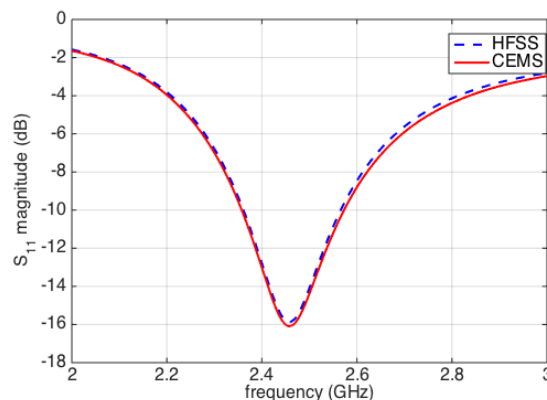

Fig. 2. The comparison of S_{11} parameter of the printed antenna from HFSS and CEMS.

The 2D gain patterns for θ and φ polarizations in xy, xz, and yz planes at 2.46 GHz are presented in Fig. 3. It is shown that the dipole is an omni-directional antenna and the maximum gain is 2.28 dB. In addition, the gain for φ polarization in these three planes are all below -15 dB, which implies that the printed dipole is mainly a linearly polarized antenna.

(a)

(b)
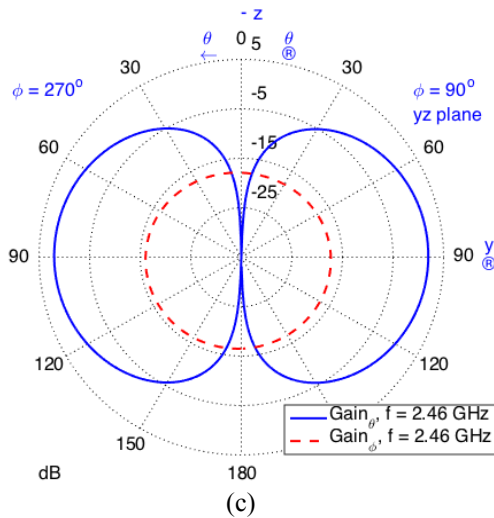

Fig. 1. Front view (a) and back view (b) of the printed dipole. The unit of all dimensions is mm.

(c)
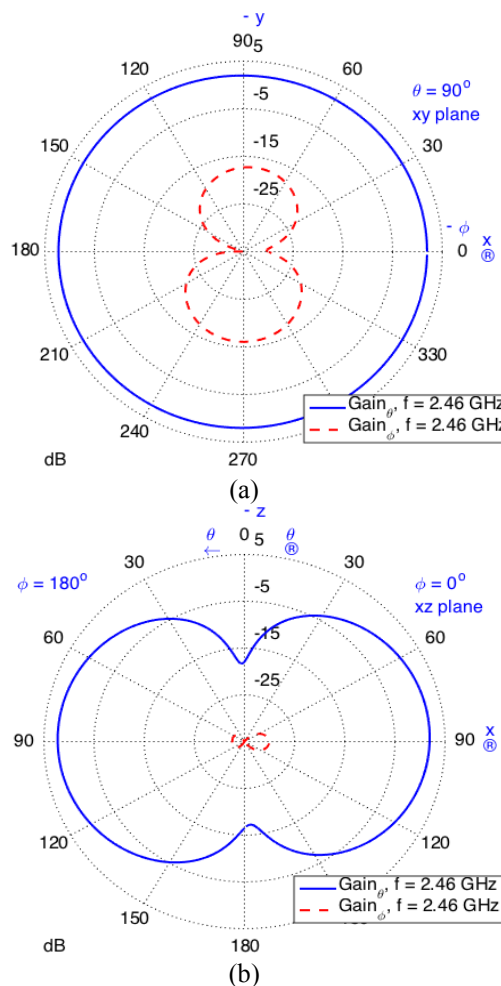
Fig. 3. The gain patterns of printed dipole for θ and φ polarizations at 2.46 GHz: *xy* plane, *xz* plane and *yz* plane are shown in (a), (b) and (c) respectively.

III. MEANDER ANTENNA

Although the printed dipole operates at 2.46 GHz, the size of the dipole arm should be reduced to get a better miniaturization. On the basis of the printed dipole, a meander antenna with a smaller size operating at 2.46 GHz is presented in this section.

The front and back view of the meander antenna are shown in Figs. 4 (a) and (b) respectively. The meander antenna is printed on a substrate with dimensions of 50 mm × 50 mm × 0.75 mm. The relative permittivity of the substrate is ε_r=2.2. Two design parameters, L denoting the width of the meandered strip and G denoting the width of the gaps, have the largest effect on the bandwidth and are chosen to be optimized for the antenna to work on the desired operating frequency.

Firstly, the cases of meander antenna with different widths of strip line are simulated. The width of the strip line increases from 0.5 mm to 1.5 mm with step of 0.25 mm. The return loss is shown in Fig. 5, from which we can see that as the width of the meandered strip increases, the bandwidth increases a little bit. Therefore, 1.5 mm is chosen as the width of the strip in order to obtain a larger bandwidth. Then, we conduct the simulations with different gap widths from 1.5 mm to 2 mm, which aims to keep the resonant frequency at 2.46 GHz. Finally, we choose 1.8 mm as the width of the gap. The return loss of the meander dipole with different gap widths are shown in Fig. 6. The length of the antenna arm with different L and G are shown in Table 1.

According to the simulation results above, the strips in the meander part are set to be 1.5 mm wide, and the gaps are set to be 1.8 mm wide. Each arm of the meander antenna is 18.4 mm long.
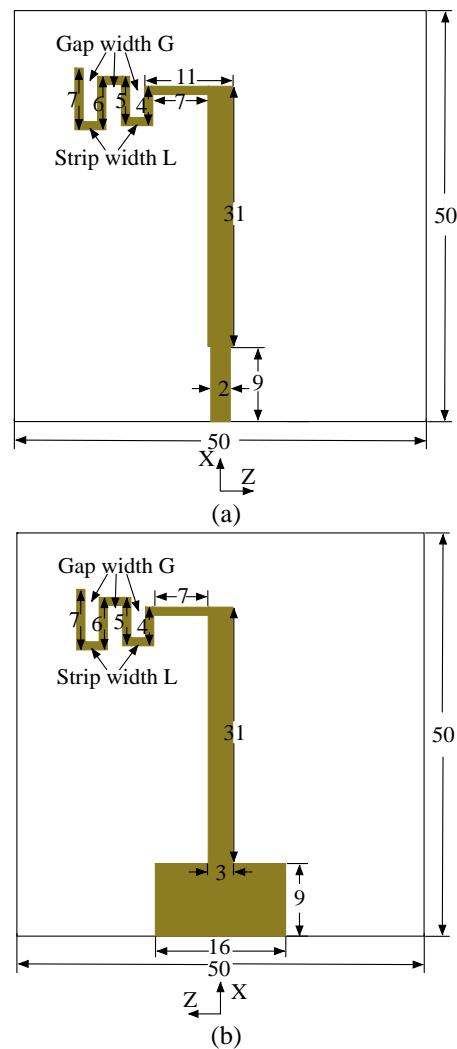

(a)

(b)

Fig. 4. Front view (a) and back view (b) of the meander antenna. The unit of all dimensions is mm.

Table 1: The length of the meander dipole arm with different strip width and gap width

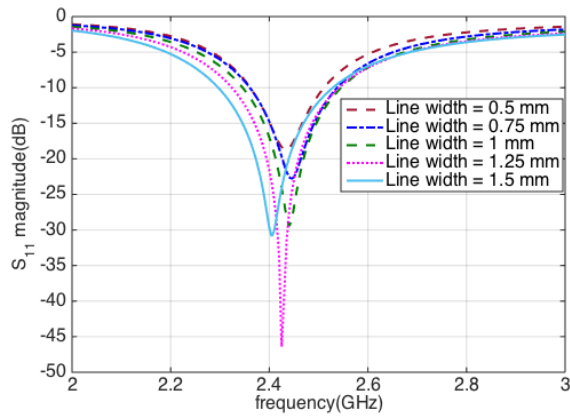| Strip Width (L)	Gap Width (G)	Arm Length
0.5 mm	1.8 mm	14.4 mm
0.75 mm	1.8 mm	15.4 mm
1 mm	1.8 mm	16.4 mm
1.25 mm	1.8 mm	17.4 mm
1.5 mm	1.8 mm	18.4 mm
0.5 mm	2 mm	15 mm
0.75 mm	2 mm	16 mm
1 mm	2 mm	17 mm
1.25 mm	2 mm	18 mm
1.5 mm	2 mm	19 mm

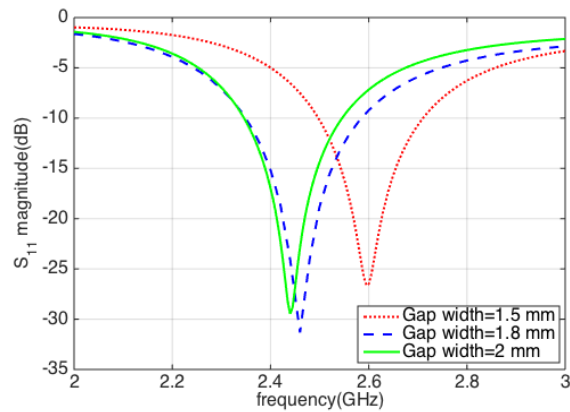Fig. 5. Return loss of meander antenna with different widths of the strip.

Fig. 6. Return loss of meander antenna with different widths of gap.

The design of the optimised meander antenna is also verified by CEMS. Return loss of meander antenna from HFSS and CEMS are shown in Fig. 7. The results from these two software match very well.
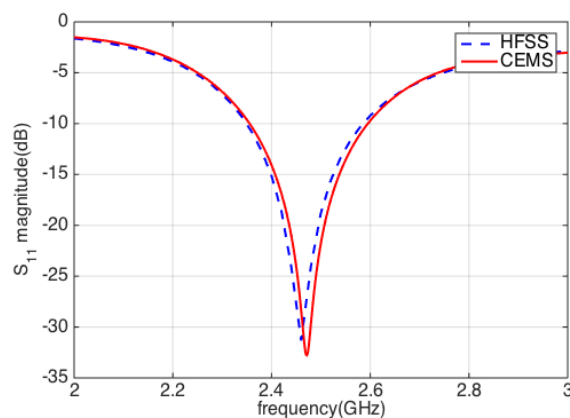

Fig. 7. The results of S_{11} parameter of optimized meander antenna from HFSS and CEMS.

As it is shown in Table 2, the operating frequency of printed dipole and meander antenna are the same. However, the design of this meander antenna allows a reduction of the antenna size. Compared to the arm length 24.5 mm of the printed dipole, the reduction of the size of the meander antenna arm is 24.89%.

Table 2: The frequency and size of printed dipole and meander antenna

Quantity	Dipole	Meander Antenna
f_{lower} /GHz	2.36	2.35
f_0 /GHz	2.46	2.46
f_{upper} /GHz	2.57	2.585
Bandwidth	8.53%	9.59%
Arm size /mm	24.5	18.4

The gain patterns for θ and φ polarizations are shown in Fig. 8. The maximum gain of the meander antenna is 2.2 dB, the same as that of the printed antenna. The gain of φ orientation on these three planes are all below -15 dB, which indicates the linear polarization of the meander antenna.
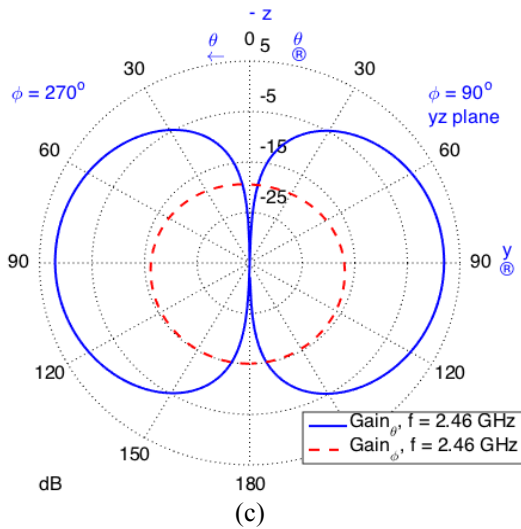

(a)

(b)

(c)
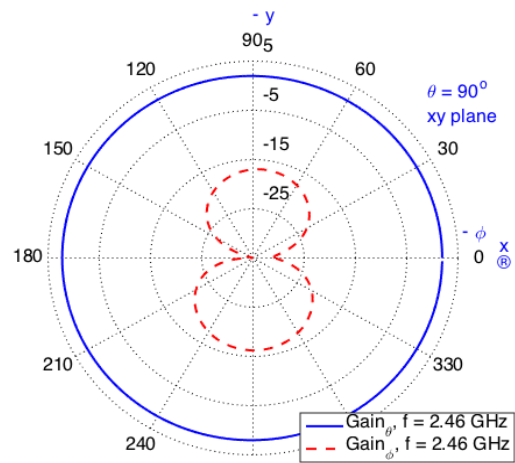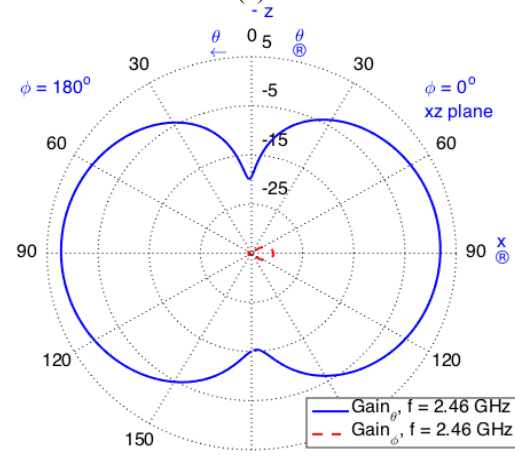
Fig. 8. The gain patterns of meander antenna for θ and φ polarizations at 2.46 GHz: xy plane, xz plane and yz plane are shown in (a), (b) and (c) respectively.

IV. MEANDER LOOP ANTENNA

Compared to the printed dipole, the design of the meander antenna reduces the size of the antenna. However, a better bandwidth of the antenna is desired. So in this part we aim to do an optimization to the meander antenna to obtain a wider frequency band without big change in antenna size.

After trying several configurations of the antenna, the geometry model of the meander loop antenna which has a larger bandwidth is finally obtained. In this design, the antenna arm is a meander loop consisting the upper meander part and the lower meander part, as shown in Fig. 9. The dimensions of the substrate are also 50 mm × 50 mm × 0.75 mm. The loop configuration is similar to the wideband design of anti-pedal bow-tie antennas operating in the C and X bands [8].
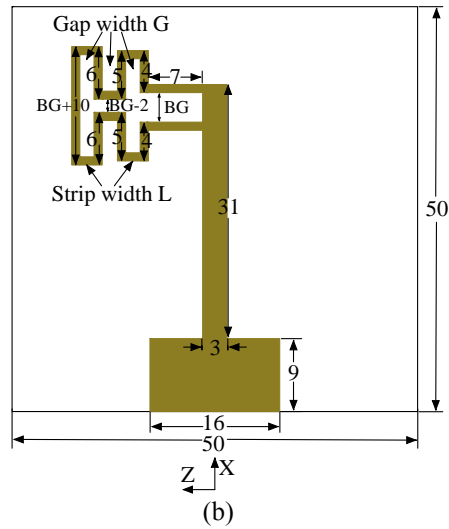

(a)

(b)

Fig. 9. Front view (a) and back view (b) of the meander loop antenna. The unit of all dimensions is mm.

The parameter BG denoting the distance between the upper and lower meander part is optimized first. Widths of gaps and strips of the meander loop antenna are 1.8 mm and 1.5 mm, respectively, which are the optimized values of the meander antenna mentioned in Section III. Different values of BG slightly affect the bandwidth of the meander loop antenna, and a better bandwidth is obtained when the value of BG is 2.75 mm. While the value of BG changes, the resonant frequency of the antenna almost keeps the same value at 2.6 GHz, as is shown in Fig. 10.

Since the desired resonant frequency of the antenna is 2.6 GHz, further work should be done in order to let the resonant frequency go back to 2.46 GHz. Therefore, models of the meander loop antenna with different gap widths (GL) are simulated in this part. The width of the gap is 1.8 mm in the optimization of BG, and we increased the width to 2.1 mm, 2.3 mm and 2.5 mm respectively in the new geometry models. The S_{11} parameter curves of different gap widths are shown in Fig. 11, in which we can see that as the gap width increases, the resonant frequency goes down. The resonant frequency is 2.46 GHz when the gap width is 2.3 mm. The length of the arm of the meander loop dipole is shown in Table 3.

In order to verify the simulation results from HFSS, the optimized meander loop antenna is also simulated by CEMS. The S_{11} curves of the optimized meander loop antenna from HFSS and CEMS are shown in Fig. 12. The results show that the curves have a good match, which indicates the accuracy of the simulation results of the meander loop antenna.

The meander loop antenna has the same resonant frequency as the dipole antenna and meander antenna. However, the meander loop antenna has a larger
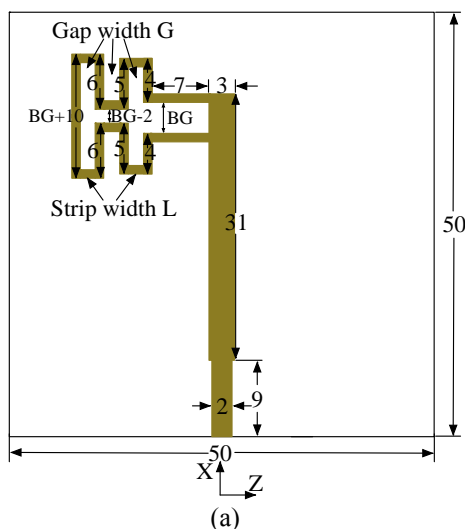
bandwidth. The comparison of arm sizes, operating frequencies and bandwidths of these three antennas are shown in Table 2. f_{lower}, f_{upper} and f_0 represent the minimum, maximum and resonant frequency, respectively. From the results in the Table 4, we can see that the meander loop antenna has a 18.7% reduction in size and a 47.7% increase in bandwidth compared to the dipole antenna.
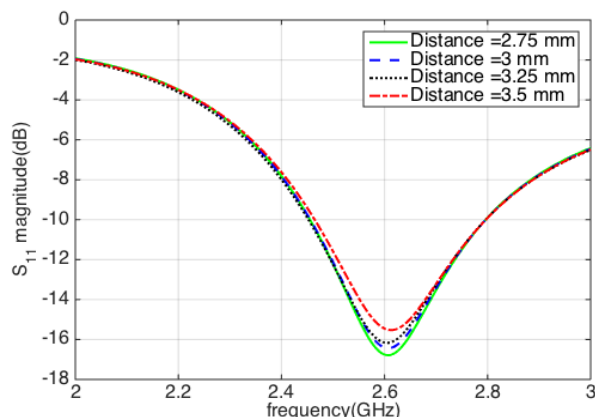

Fig. 10. S_{11} parameter curves of meander loop antenna with different distance between the upper meander part and the lower meander part.

Table 3: The length of the arm of the meander loop dipole with different gap width

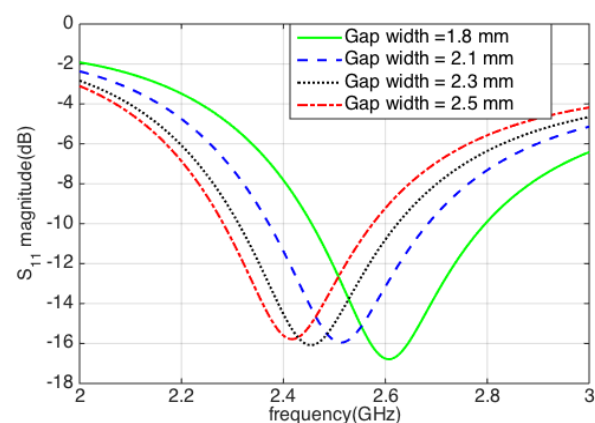| Gap Width (GL)	Loop Distance (BG)	Arm Length
1.8 mm	2.75 mm	18.4 mm
2.1 mm	2.75 mm	19.3 mm
2.3 mm	2.75 mm	19.9 mm
2.5 mm	2.75 mm	20.5 mm

Fig. 11. The S_{11} curves of meander loop meander with different gap width.
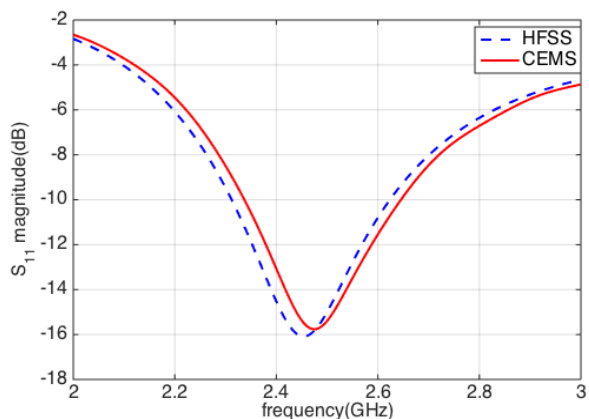

Fig. 12. The comparison of S_{11} curves of optimized meander loop antenna from HFSS and CEMS.

Table 4: The operating frequencies and arm size of these three antennas

Quantity	Dipole Antenna	Meander Antenna	Meander Loop Antenna
f_{lower} /GHz	2.36	2.35	2.315
f_0 /GHz	2.46	2.46	2.46
f_{upper} /GHz	2.57	2.585	2.625
Bandwidth	8.53%	9.59%	12.6%
Arm size /mm	24.5	18.4	19.9

The gain patterns for θ and φ polarizations of the meander loop antenna are shown in Fig. 13. It is shown from these patterns that the maximum gain of the meander loop antenna is 2.16 dB and the gain in φ polarization in these three planes are all below -15 dB, which indicates the meander loop antenna is also linearly polarized.
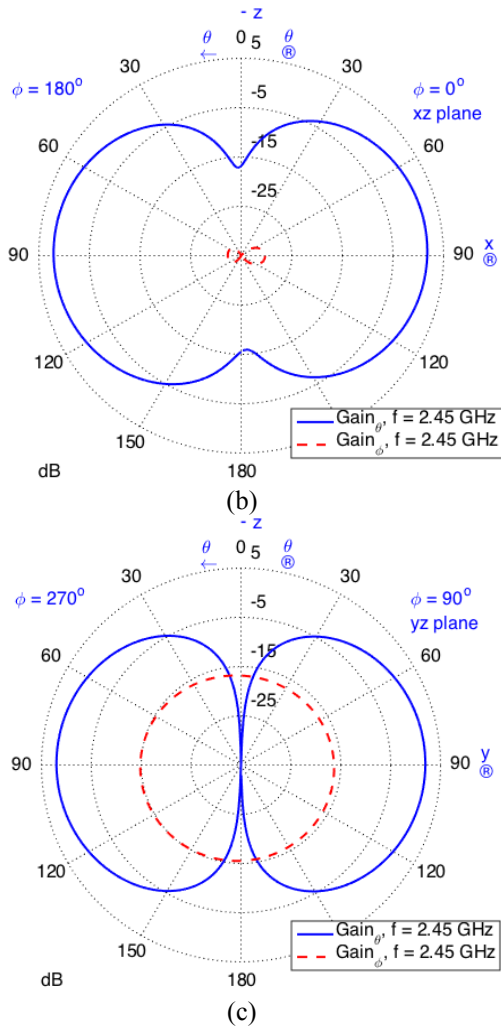

(a)

(b)

(c)
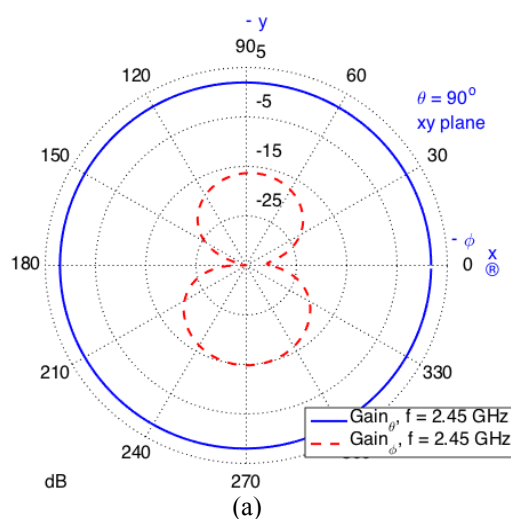
Fig. 13. The gain patterns of meander loop antenna for θ and φ polarizations at 2.45 GHz: *xy* plane, *xz* plane and *yz* plane are shown in (a), (b) and (c) respectively.

V. FABRICATION AND MEASUREMENT

The fabrication and measurement of the printed dipole, meander antenna, and meander loop antenna are presented in this part. The printed dipole is shown in Fig. 14 (a), the dimensions of the substrate is 62 mm × 50 mm. The meander antenna with L=1.5 mm and G=1.8 mm is shown in Fig. 14 (b). The loop meander dipole with L=1.5 mm, G=2.3 mm and BG=2.7 mm is shown in Fig. 14 (c). The dimensions of the substrate of meander dipole and meander loop dipole are 50 mm × 50 mm × 0.75 mm. The relative permittivity of the substrate of all the antennas is ε_r=2.2.

The measurements of the S_{11} parameter of these three antennas are shown in Fig. 15. The measurements of these three antennas in terms of the operating frequency and resonant frequency are shown in Table 5.

From Fig. 15, Table 4 and Table 5 we can see that the simulation results and measurements are in good agreement for the printed dipole and the meander antenna. Slight deviation is observed between simulated and measured results for the meander loop antenna, which could be attributed to unexpected tolerances in fabrication due to the more complicated structure of the its arm. Compared to the dipole antenna, the meander antenna and the meander loop antenna both have larger bandwidth, and the bandwidth of the meander loop antenna is the largest. Based on the measurement results, the bandwidth of the meander antenna and meander loop antenna increase by 21.1% and 54.5% respectively.
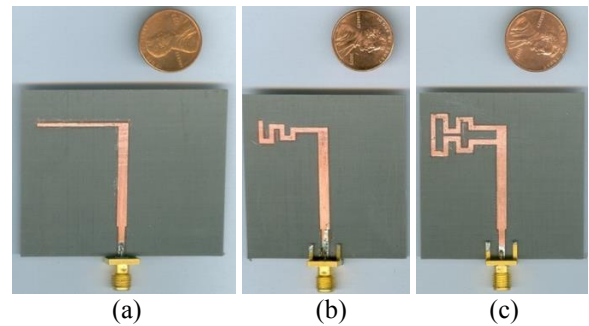

(a)   (b)   (c)

Fig. 14 The picture of printed dipole (a), meander antenna (b), and meander loop antenna (c).

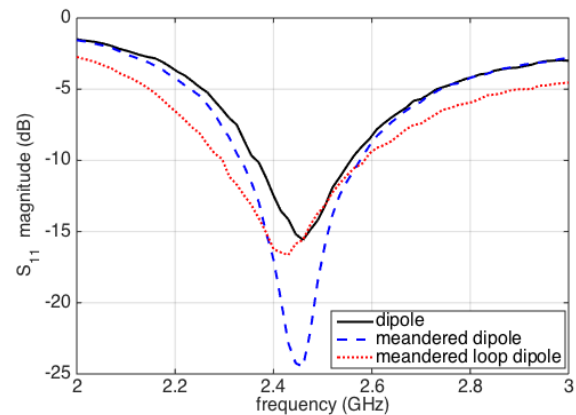Fig. 15. The measurements of S_{11} parameter of three antennas.

Table 5: The operating frequencies of three antennas from measurements

Quantity	Dipole Antenna	Meander Antenna	Meander Loop Antenna
f_{lower} /GHz	2.36	2.34	2.30
f_0 /GHz	2.46	2.46	2.43
f_{upper} /GHz	2.55	2.57	2.59
Bandwidth	7.72%	9.35%	11.93%

VI. CONCLUSION

The three antennas including a printed dipole, a meander antenna, and a meander loop antenna used in the wireless communication system with center frequency of 2.46 GHz are presented in this research. Based on the design of the first printed dipole, the miniaturization of the dipole is obtained by meandering the dipole arm and the bandwidth of the dipole is enhanced by the design of the meander loop. The choice of parameters for each design and the process of the optimization of these three antennas are presented in details one after another. The models of these antennas are simulated by HFSS and verified by CEMS and the simulation results fit well. These three antennas are fabricated and measured and the measurements of the return loss have a good match with the simulated results. From these results it is shown that, compared to the printed dipole, the meander antenna and meander loop antenna both have approximately 19% reduction in the size of the antenna. In addition, the 10 dB bandwidth of both designs increases. Especially the meander loop antenna has an approximately 50% increase in bandwidth compared to the traditional printed dipole.

REFERENCES

[1] C. Soras, M. Karaboikis, G. Tsachtsiris, and V. Makios, "Analysis and design of an inverted-F antenna printed on a PCMCIA card for the 2.4 GHz ISM band," *IEEE Antennas and Propagation Magazine*, vol. 44, no. 1, pp. 37-44, 2002.

[2] C. C. Lin, L. C. Kuo, and H. R. Chuang, "A horizontally polarized omnidirectional printed antenna for WLAN applications," *IEEE Transactions on Antennas and Propagation*, vol. 54, no. 11, pp. 3551-3556, 2006.

[3] H. Ma and H. Y. D. Yang, "Miniaturized integrated folded helical antennas," in *2011 IEEE International Symposium on Antennas and Propagation (APSURSI)*, pp. 753-756, 2011.

[4] C. M. Allen, A. Z. Elsherbeni, C. E. Smith, C. W. P. Huang, and K. F. Lee, "Tapered meander slot antenna for dual band personal wireless communication systems," *Microwave & Optical Technology Letters*, vol. 36, no. 5, pp. 381-385, 2003.

[5] J. Rashed and C. T. Tai, "A new class of resonant antennas," *IEEE Transactions on Antennas and Propagation*, vol. 39, no. 9, pp. 1428-1430, 1991.

[6] Y. Zhang and H. Y. D. Yang, "Bandwidth-enhanced electrically small printed folded dipoles," *IEEE Antennas and Wireless Propagation Letters*, vol. 9, pp. 236-239, 2010.

[7] A. Z. Elsherbeni and V. Demir, *The Finite-Difference Time-Domain Method For Electromagnetics with MATLAB Simulations*. 2nd edition, Edison, NJ: SciTech Publishing, an Imprint of the IET, 2016.

[8] A. A. Eldek, A. Z. Elsherbeni, and C. E. Smith, "Wide-band modified printed bow-tie antenna with single and dual polarization for C - and X-band applications," *IEEE Transactions on Antennas and Propagation*, vol. 53, no. 9, pp. 3067-3072, 2005.